Crystal Packing and Molecular Dynamics Studies of the 5-Nitro-2,4-dihydro-3*H*-1,2,4-triazol-3-one Crystal

Dan C. Sorescu[†] **and Donald L. Thompson***

Department of Chemistry, Oklahoma State University, Stillwater, Oklahoma 74078

Received: January 8, 1997; In Final Form: February 26, 1997[⊗]

We have developed an intermolecular potential to describe the β-structure of the 5-nitro-2,4-dihydro-3*H*-1,2,4-triazol-3-one (NTO) crystal in the approximation of rigid molecules. The potential is composed by pairwise Lennard-Jones, hydrogen-bonding terms and Coulombic interactions. Crystal-packing calculations performed with the proposed potential acceptably reproduce the main crystallographic features of the crystal and yield very good agreement with the estimated lattice energy. These findings are also supported by the results of isothermal−isobaric molecular dynamics (MD) simulations at zero pressure for temperatures ranging from 4.2 to 400 K. Throughout the MD simulations the average structure of the crystal maintains the same space group symmetry as the one determined experimentally. The thermal expansion coefficients calculated for the model indicate anisotropic behavior.

I. Introduction

The behavior of crystalline 5-nitro-2,4-dihydro-3*H*-1,2,4-triazol-3-one (NTO) under thermal and radiative conditions has been the subject of a number of studies in recent years.[1−8] Most of these studies have focused on the thermal decomposition of NTO, and a variety of mechanisms have been proposed. These include an autocatalytic mechanism,[1] nitrogen−hydrogen bond cleavage,[2] NO_2 elimination with formation of amide fragments,[3,4] hydrogen transfer to the nitro groups followed by subsequent loss of HONO,[6] and bimolecular oxygenation of the carbonyl group by the nitro group of an adjacent NTO molecule.[8] This variety of mechanisms illustrate the need for additional theoretical and experimental studies to determine the influence of the physical state of the reacting material and the reaction conditions if we are to understand NTO decomposition.

In a previous paper[9] we reported experimental and theoretical studies of the geometric and spectroscopic parameters for NTO in the gas and solid phases. In particular, the structure of the NTO molecule in the gas phase was determined by *ab initio* molecular orbital calculations at the Hartree−Fock and second-order Møller−Plesset (MP2)[10] levels and by density functional theory with Becke's three-parameter hybrid method[11] in combination with the Lee, Yang, and Parr correlation functional (B3LYP),[12] using different types of basis sets ranging from 3-21G[13] to 6-311G**.[14] The fundamental vibrational frequencies for optimized geometries were calculated using analytical second derivatives. The MP2/6-311G** *ab initio* frequencies are in good agreement with the experimental values obtained by recording the IR spectra of NTO isolated in an argon matrix at 21 K. These spectra consist of well-defined, narrow infrared bands, indicating minimal intermolecular interactions. We also investigated how the spectral features of NTO are influenced by environment by measuring the spectrum of a thin film of pure NTO.[9] This spectrum is significantly different from those for NTO isolated in an argon matrix. Indeed, the infrared bands exhibit extensive broadening and large frequency shifts due to strong intermolecular interactions in the polycrystalline phase. The *ab initio* and the experimental results for geometries and fundamental frequencies were used to develop two intramolecular force fields, one for gas-phase NTO and the second for NTO in the crystalline phase.[9]

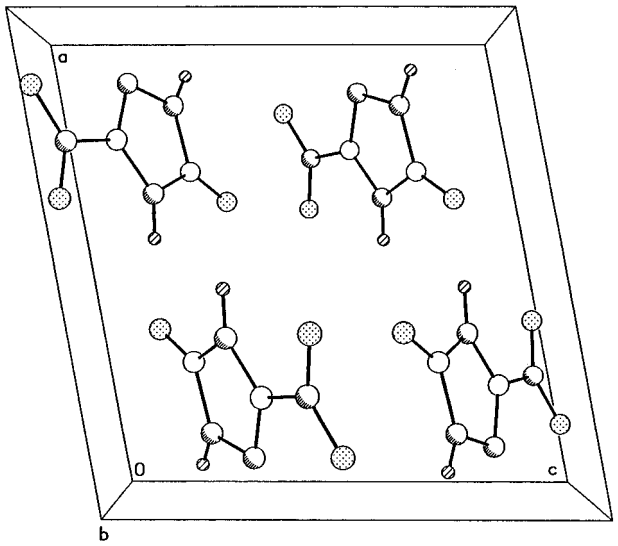

Figure 1. Unit cell of the β-NTO crystal. The coordinates are taken from Lee and Gilardi, ref 15.

In the present study we focus on the analysis of the intermolecular interactions in solid phase NTO. It is known that crystalline NTO exists in two phases, α and β.[15] The first one is the most stable. It belongs to the triclinic space group $P1$ and contains eight molecules in the unit cell. However, attempts to determine the coordinates of individual atoms for this structure have not been successful due to "some kind of twinning about the crystal needle axis".[15] The β-phase has been resolved by X-ray diffraction measurements.[15] The unit cell is monoclinic with four molecules in the unit cell and has the space group $P2_1/c$ (see Figure 1). Due to the availability of a full set of experimental bond lengths and angles for this phase, we have considered it in both our previous[9] and present studies.

The main objective of the work reported in the present paper is to extend our previous study of the intramolecular force field of NTO in the gas and crystalline phases[9] by developing an intermolecular potential for the β-NTO crystal. Such a potential will allow direct theoretical investigations of the response of

[†] Current mailing address: Department of Chemistry, University of Pittsburgh, Pittsburgh, PA 15260.

[⊗] Abstract published in *Advance ACS Abstracts,* April 15, 1997.

S1089-5647(97)00128-4 CCC: $14.00

NTO crystals to different external stimuli such as heating or pressure. This information can be further used to determine the optimum conditions for manipulation and control of the behavior of this material.

The methodology followed to develop the intermolecular potential is similar to that used previously for the hexahydro-1,3,5-*s*-triazine (RDX) crystal.[16] Basically the intermolecular interactions are assumed to be describable by simple isotropic potentials such as the (6-exp) Buckingham potentials or the (6-m) Lennard-Jones potentials with explicit consideration of the electrostatic interactions between the charges associated with various atoms of different molecules. The parametrization of the potential function is done such that the model reproduces the experimental structure of the crystal and its lattice energy. In more elaborate cases, the elastic properties of the crystal and the phonon frequencies can also be considered in the fit of repulsion and dispersion potential parameters. The validity of this approach based on the use of (6-exp-1) or (6-m-1) potentials has been demonstrated in numerous studies of organic molecular crystals,[17,18] and several sets of empirical intermolecular potentials such as Amber,[19] ECEPP,[20] and Dreiding[21] are available for simulating organic, biological, and main-group inorganic crystals.

We find that for NTO the crystalline structure and its energy can be reasonably predicted by using a superposition of Coulombic terms, 6−12 Lennard-Jones potentials, and 10−12 potentials to describe the hydrogen bonding. The Coulombic terms were determined by fitting partial charges centered on each atom of the NTO molecule to a quantum mechanically derived electrostatic potential. Excepting the intermolecular parameters used to describe the N−H···O═C hydrogen bonds, the other homo- and heteroatom potential parameters were taken from previously published studies. The N−H···O═C parameters were selected such that the structure and its energy obtained from symmetry-unconstrained molecular packing calculations reproduce the corresponding experimental values. In all these calculations the molecules are assumed to be rigid and the structure is described by the center of mass positions and the orientational parameters (the Euler angles or the set of quaternions) for each molecule in the unit cell. The intermolecular potential determined in molecular packing calculations was further tested in isothermal−isobaric molecular dynamics calculations (NPT-MD) at zero pressure as a function of temperature over the range 4.2−400 K.

The organization of the paper is as follows: In section II we present the intermolecular potential used to describe the NTO crystal and brief descriptions of the molecular packing and NPT-MD methods. In section III we present the results of lattice energy minimization by molecular packing calculations without symmetry constraints followed by the results of the trajectories calculations for the NPT ensemble. Finally, we summarize the main conclusions in section IV.

II. The Method

A. Molecular Packing Calculations. A general procedure for testing empirical or semiempirical intermolecular potential energy functions for organic crystals is the use of molecular packing calculations.[17,22−24] The basic idea consists of minimization of the lattice energy with respect to the structural degrees of freedom of the crystal. For a crystal with Z rigid molecules per unit cell, these degrees of freedom are determined by the positions and orientations of the molecules in the unit cell as well as the dimensions and angles of the unit cell.

Significant reduction of the computational time necessary to minimize the lattice energy starting with a trial configuration can be obtained by imposing and maintaining the observed space group symmetry of the crystal throughout energy minimization. There are available several molecular packing packages such as WMIN[22] or PCK91[24] that use this type of minimization procedure. However, studies done by Hagler and co-workers[25] and more recently by Gibson and Scheraga[28] show that maintenance of the observed space group symmetry, after energy minimization, should be considered a necessary condition in assessing the accuracy of the empirical potential energy. We have reached a similar conclusion in a study of the RDX crystal;[16] that is for an accurate force field for a crystal, there are no significant differences when the minimization of the lattice energy is done using space group symmetry constraints and when these constraints are removed.

In the present study we have chosen to use the method of crystal packing calculations without symmetry constraints. This can be done using the algorithm proposed by Gibson and Scheraga[26] for efficient minimization of the energy of a fully variable lattice composed of rigid molecules and implemented in the LMIN[27] program. This algorithm makes use of Gay's[28] secant-type unconstrained minimization solver (SUMSL routine) to minimize the lattice energy. The gradients of the energy with respect to generalized coordinates, *i.e.*, the $6Z$ rigid-body parameters of the Z molecules in the unit cell and the six lattice parameters, are evaluated analytically.

The potential function used to describe the NTO intermolecular interactions was constructed as a sum of pairwise additive Lennard-Jones (LJ), hydrogen-bonding (HB), and Coulombic (C) potentials of the form

$$V_{\alpha\beta}^{\mathrm{LJ}}(r) = \epsilon_{\alpha\beta}^{0}\left[\left(\frac{r_{\alpha\beta}^{0}}{r}\right)^{12} - 2\left(\frac{r_{\alpha\beta}^{0}}{r}\right)^{6}\right] \tag{1}$$

$$V_{\alpha\beta}^{\mathrm{HB}}(r) = \epsilon_{\alpha\beta}^{0}\left[5\left(\frac{r_{\alpha\beta}^{0}}{r}\right)^{12} - 2\left(\frac{r_{\alpha\beta}^{0}}{r}\right)^{10}\right] \tag{2}$$

and

$$V_{\alpha\beta}^{c}(r) = \frac{q_\alpha q_\beta}{4\pi\epsilon_0 r} \tag{3}$$

where $\epsilon_{\alpha\beta}^{0}$ is the energy minimum for the pair of atoms α and β, $r_{\alpha\beta}^{0}$ is the interatomic distance at the energy minimum, q_α and q_β are the electrostatic charges on the atoms, and ϵ_0 is the dielectric permittivity constant for vacuum.

Based on eqs 1−3 the lattice energy can be evaluated as the sum of interactions between the molecules in the central unit and all the other molecules in the image cells. For practical computational purposes, the lattice sums are evaluated over cells within a sphere centered at the origin and of radius limited by the chosen cutoff distance. In order to ensure the continuity of the energy and its first derivative, both the LJ and HB interactions are cut off at a distance Qr^0 using a cubic feather (spline) applied over the distance $Pr^0 - Qr^0$. Here, the P and Q parameters specify, respectively, the start and the end of the feather and represent the multiplicative coefficients for the interatomic distance r^0 at the energy minimum. In all our calculations the parameter P was set equal to Q-0.5. The influence of different cutoff distances on the final lattice parameters will be discussed in the following sections.

The evaluation of the Coulombic sums over the infinite periodic lattice has been done using the standard Ewald's transformation technique[16,26] to improve the slow rate of convergence of these sums. Further details of the summations procedures of different energy terms over the lattice as well as of the adjustable parameter that determines the relative contribution of the direct and reciprocal-space terms in the Ewald sum are given in ref 26.

As the purpose of our calculations was to determine the best parametrization of the potential parameters to describe the NTO crystal, the experimentally observed geometry[10] was taken as the starting point for energy minimization. The orientation of the molecules with respect to the Cartesian space-fixed system was described by setting the origin of the body-fixed coordinates at the centroids of the molecules and with the axes aligned along the principal axes of inertia, with unit weight assigned to each atom.[26] During energy minimization, the values of the translational vectors, describing the origin of the centroids, and of the Euler angles, representing the orientations of the molecules, give the necessary information on the relative positions of the molecules in the unit cell.

In order to determine the space group symmetry of the crystal predicted by the semiempirical potential, at the beginning and at the end of the lattice energy minimization the symmetry operations that transform the molecules in the unit cell are computed. The space group is considered to be conserved if the symmetry operations, as defined in the International Tables of Crystallography,[29] between a given molecule and the remaining molecules in the unit cell remain unchanged and if the lattice parameters fixed by the lattice symmetry have not been modified significantly. If the space symmetry is not conserved as a result of energy minimization, a new space group is deduced on the basis of the final symmetry relations. It has been shown[26] for the cases when the space group symmetry remains unchanged that some of the symmetry transformations may be lost during energy minimization, but they are regained before convergence takes place. In the particular case of the β-NTO crystal, with space group $P2_1/c$, the angles α and γ of the unit cell are fixed at 90° by space group symmetry.

As mentioned before, the optimum set of potential parameters should minimize the differences between the predicted and experimental geometry of the crystal. In addition we imposed the condition that the calculated energy match the static lattice energy U^0 of the crystal. This quantity can be estimated from the experimental enthalpy of sublimation using the relation[30] $-\Delta H^{sub} = U^0 + K_0 + 2RT$, where K_0 is the zero-point energy and the factor $2RT$ is due to the difference of molar heat capacities between solid ($6R$) and gas ($3R$) and to the expansion work of a mole of gas, in the approximation of an ideal gas ($PV = RT$). We have made the assumption that the static lattice energy can be calculated from the sublimation enthalpy with inclusion of the $2RT$ factor but neglecting the zero-point energy.

To the best of our knowledge an experimental value for the enthalpy of sublimation of NTO has not been published; however, an approximate value can be determined using the known values of the enthalpies of formation of gas and solid phases by using the relation

$$\Delta H_{sub} = \Delta H_{f(gas)} - \Delta H_{f(solid)} \tag{4}$$

Two different values are available for the enthalpies of formation of NTO in the gas phase. The first one, $\Delta H_{f\ (gas)} = -3.2$ kcal/mol has been obtained by Ritchie[31] based on the calculated Hartree−Fock HF/6-31G*//3-21G energy of a single molecule and the group equivalents of Ibrahim and Schleger.[32] A second value of −5.7 kcal/mol has been determined recently by Politzer *et al.*[33] based on a nonlocal density functional procedure with empirical correction terms. Using these values for $\Delta H_{f(gas)}$ and the experimental number $\Delta H_{f(solid)} = -30.927$ kcal/mol obtained by Finch and co-workers,[34] a lattice energy of −110.46 or −121.02 kJ/mol can be estimated, with inclusion of the $2RT$ term. For our molecular packing calculations we considered the average of the above lattice energies, *i.e.*, $U^0 = -115.74$ kJ/mol.

TABLE 1: Electrostatic Charges for the NTO Molecule Determined by the CHELPG Procedure at the MP2/6-31G Level**

atom[a]	charge/|*e*|
N_1	−0.412 881
N_2	−0.133 939
C_3	0.532 072
N_4	−0.417 327
C_5	0.369 819
N_6	0.610 409
O_7	−0.334 555
O_8	−0.370 087
O_9	−0.517 071
H_{10}	0.320 576
H_{11}	0.352 984

[a] The atom designation numbers are defined in Figure 2.

The assignment of the electrostatic charges poses a problem in that the atom-centered monopole charge is not an observable quantity and cannot be obtained directly from either experiment or *ab initio* calculations. There are several schemes for evaluation of charges by empirical partition or by using a quantum mechanically derived wave function.[35] We have chosen to make the assignments for the atom-centered monopole charges by using the set that best reproduces the quantum mechanically derived electrostatic potential that is calculated over grid points surrounding the van der Waals surface of the NTO molecule. This method of fitting to the electrostatic potential was proposed by Breneman and Wiberg[36] and is incorporated in the Gaussian 94 package of programs[37] under the keyword CHELPG. This method presents the advantages of having a higher density of points and a better selection procedure, which ensures a decrease of rotational variables observed with other methods. We have used this method in conjunction with Møller−Plesset perturbation theory at the MP2/6-31G** level.[10,38] The atomic arrangement of the molecule used in these calculations is consistent with the crystallographic configuration.[15] A total number of 8366 points were used in the fit, leading to a root-mean-square deviation of 0.003 02. The resulting electrostatic charges are given in Table 1.

The parameters for the NTO intermolecular potential in eqs1 and 2 are those previously published by Gibson and Scheraga,[26] with the exception of the N−H···O═C hydrogen bond potential. The potential parameters for that case have been optimized to minimize the differences between the predicted and experimental geometries as well as their corresponding energies. Indeed, large rotations of the molecules inside the unit cell were observed in the lattice energy minimization procedure when the original set of parameteres for N−H···O═C hydrogen bonding given in ref 26 were used. These rotations were decreased by adjusting the values of the parameters ϵ^0 and r^0 of the N−H···O═C hydrogen bond potential. For calculation of the heteroatom parameters from homoatom parameters we have used the combination rule suggested by Scheraga:[26]

$$\epsilon^0_{\alpha\beta} = \sqrt{\epsilon^0_{\alpha\alpha}\epsilon^0_{\beta\beta}}\frac{(r^0_{\alpha\alpha} + r^0_{\beta\beta})^3}{(r^0_{\alpha\beta})^6} \tag{5}$$

where

$$r^0_{\alpha\beta} = \frac{1}{2}(r^0_{\alpha\alpha} + r^0_{\beta\beta}) \tag{6}$$

The full list of potential parameters used in our calculations is given in Table 2.

B. Constant Pressure and Temperature Molecular Dynamics Calculations. A more comprehensive test of the

TABLE 2: NTO Atom−Atom Potential Parameters

pair ($\alpha-\beta$)	$\epsilon^0_{\alpha\beta}$ (kcal/mol)	$r^0_{\alpha\beta}$ (Å)
Lennard-Jones[a]		
N_1-N_1	0.067 39	3.89
N_2-N_2		
N_4-N_4	0.052 14	4.06
N_6-N_6		
C_3-C_3	0.106 18	3.61
C_5-C_5	0.107 97	3.912
O_7-O_7	0.203 98	2.97
O_8-O_8		
O_9-O_9	0.217 39	3.07
$H_{10}-H_{10}$	0.051 00	2.43
$H_{11}-H_{11}$		
hydrogen bonding		
N−H···O═C	2.600 000	1.800 000
N−H···O−N	1.478 869	1.879 022

[a] The values of the parameters $\epsilon^0_{\alpha\beta}$ and $r^0_{\alpha\beta}$ for pairs of unlike atoms are calculated by using eqs 5 and 6.

intermolecular potential for the NTO crystal was done with a constant pressure and temperature (NPT) molecular dynamics simulation, in which there are no geometric constraints other than the assumption of rigid-body molecules. This method yields average equilibrium properties of the lattice as functions of temperature and pressure.

For systems that evolve under constant temperature and pressure, Andersen[39] introduced a new Lagrangian formulation in which the volume of the system is considered a variable, the time evolution of which is determined by the imbalance between the internal and external fixed pressure. Later, Parrinello and Rahman[40] extended this approach to allow both isotropic and anisotropic volume changes under an external applied hydrostatic pressure or a general stress tensor. Their method proved to be well suited to the study of structural transformation in solids, and many subsequent studies have been devoted to this subject.[41] Nosé and Klein[42,43] extended the method of molecular dynamics for constant numbers of particles, pressure, and temperature (NPT-MD) to treat both molecular and ionic systems. They also showed how the long-range charge−charge interactions can be included in the general formalism.[42]

We have used the algorithm proposed by Nosé and Klein,[41] as implemented in the program MDCSPC4B,[44] to simulate the NTO crystal at various temperatures in the range 4.2−400 K and at zero pressure. The original program was modified to include hydrogen bonding as given in eq 2.

In this case, the equations of motion for both the translation of rigid molecules and the simulation cell are integrated using a fifth-order Gear predictor-corrector.[45] The molecular rotational motion is handled by using the Evans quaternion algorithm with a fourth-order Gear integrator.[46]

The MD simulation cell consists of a box containing 45 crystallographic unit cells (a $3 \times 5 \times 3$ box of unit cells). The dynamical mass parameter of the simulation cell was taken to be equal to the mass of a single NTO molecule. In the initial simulation corresponding to the lowest temperature, the position and orientation of the molecules in the unit cell were taken to be identical to those for the experimental structure. The initial velocities of the centers-of-mass of the molecules were selected at random, but modified to eliminate the translation and rotation of the bulk MD cell. The system was integrated for 11 200 time steps (1 time step $= 2 \times 10^{-15}$ s), of which 3000 steps were equilibration. In the equilibration period the velocities were scaled after every 5 steps so that the internal temperature of the crystal mimicked the imposed external temperature. Then, averaged properties were calculated over the next 8200 integration steps in the simulation. In subsequent runs, performed at successively higher temperatures, the initial configurations of the molecular positions and velocities were taken from the previous simulation at the end of the production run. The velocities were again scaled over an equilibration period of 3000 steps to achieve the desired external temperature, followed by an 8200-step production run.

The lattice sums were calculated subject to the use of minimum-image periodic boundary conditions in all dimensions in these simulations.[47] The interactions were determined between the sites (atoms) in the simulation box and the nearest-image sites within the cutoff distance ($R_{cut} = 11.5$ Å). In these calculations, the Coulombic long-range interaction was treated by using Ewald's method.[47] Also, the long-range corrections for the nonbonded potential energy and the corresponding virial were calculated by using standard techniques.[47]

Several types of calculations were performed to obtain information about structural characteristics of the crystal. First, the mean positions of the molecules in the simulation box were calculated. This was done by using the folding procedure in the MDCSPC4B program,[44] in which the molecules considered in their average positions in different subcells of the MD box are superimposed over the primitive cell. The content of these subcells is considered identical if these positions coincide within the root-mean-square deviations (rms) of their averaged values. Additional information about the structure of the crystal was obtained by calculating the center-of-mass (COM) and the site−site radial distribution functions (RDFs). Finally, the average orientations of the molecules in the unit cell were determined by evaluating the averages of the Euler angles of the principal molecular axis. The above quantities, *i.e.*, the mean positions, RDFs and Euler angles, were calculated from recordings done at every 10th step during trajectory integrations.

III. Results and Discussion

A. Molecular Packing Calculations. The results of the molecular packing calculations are summarized in Table 3 as functions of the cutoff distance parameter Q. Since evaluation of the dispersive terms of the form r^{-6} in the nonbonded potential was done without an accelerated convergence method,[16] a slight dependence of the lattice energy on the cutoff distance is expected. As can be seen from the results in Table 3, this dependence is more significant for Q values smaller than 10, above which only small variations of the total energy per molecule and of the geometrical lattice and molecular parameters take place.

For all the cases in Table 3, the symmetry space group was maintained as verified by the existent symmetry relations between different $Z - 1$ molecules in the unit cell and the central molecule, $Z = 1$. These symmetry relations are given in Table 4 and correspond to the space group $P2_1/c$.[26]

The changes in lattice and molecular parameters after energy minimization relative to the experimental structure[15] are also given in Table 3. They were calculated for $Q = 25.5$. The maximum deviations of the lattice dimensions and angles from the experimental values are 4.94% and 3.66%, respectively, and with small translations of the rigid molecules. There is essentially no change in the values of the angles α and γ, the values of which are fixed at 90° by the crystal class. However, there is a somewhat larger rotation of 5.92° for one of the Euler angles that describes the molecular orientation in the unit cell.

For the minimized lattice, the total energy is $U = -116.04$ kJ/mol. This value is in very good agreement with the value −115.74 kJ/mol, which we have estimated (see section II.A) for the static lattice energy.

TABLE 3: Lattice Parameters and Energies Obtained in Crystal Packing Calculations without Symmetry Constraints. The Percentage Change in Lattice and Molecular Parameters after Energy Minimization Is Determined as a Function of the Experimental Geometry[15]

	final energy[b]		final lattice parameters[c]					
cutoff parameter Q[a]	NB	ES	*e*	*b*	*c*	α	*β*	*γ*
3.5	−60.8606	−52.6718	9.5810	5.7921	9.0307	90.001	104.485	90.002
5.5	−62.7435	−52.7186	9.5797	5.7892	9.0223	90.000	104.486	90.000
7.5	−63.1192	−52.7243	9.5796	5.7878	9.0225	89.999	104.489	90.000
10.5	−63.2666	−52.7277	9.5796	5.7872	9.0228	90.000	104.496	90.000
20.5	−63.3367	−52.7288	9.5795	5.7870	9.0224	89.999	104.499	90.002
25.5	−63.3418	−52.7299	9.5793	5.7876	9.0217	89.997	104.489	90.001
expt			9.3260	5.5150	9.1070	90.000	101.770	90.000
Q			Δ*D*a (%)	Δ*b* (%)	Δ*c* (%)	Δa *(deg)*	Δb *(deg)*	Δg *(deg)*
25.5			2.72	4.94	−0.94	0.0	3.69	0.0
Q			Δ *x*[d]	Δ*y*	Δ*z*	ΔΦ (deg)[e]	ΔΘ (deg)	ΔΨ (deg)
25.5			−0.021	−0.001	−0.025	2.06	0.58	5.93

[a] Value of the cutoff parameter as described in the text. [b] Nonbonded (NB) and electrostatic (ES) energies per molecule in kJ/mol. [c] Lattice dimensions *a*, *b*, *c* in angstroms and angles α, *β*, *γ* in degrees. [d] Change in fractional coordinates of molecular centroids. [e] Change in Euler angles of molecular centroid.

TABLE 4: Symmetry Relations between Different Molecules in the Unit Cell and the Reference Molecule after Energy Minimization[a]

	transformation			
molecule	type[b]	axis or normal[c]	defining point[c]	translation[c]
2	2_1	(0.000,1.000,0.000)	(0.000,0.000,0.000)	(0.000,0.500,0.000)
3	1		(0.000,−0.250,0.250)	
4	g	(0.000,1.000,0.000)	(0.000,0.000,0.000)	(0.000,0.000,0.500)

[a] A complete description of these parameters is given by Gibson and Scheraga, ref 26. [b] 2_1, two-fold screw rotation; g, glide reflection; $\bar{1}$ inversion. [c] Parameters are given in fractional coordinates.

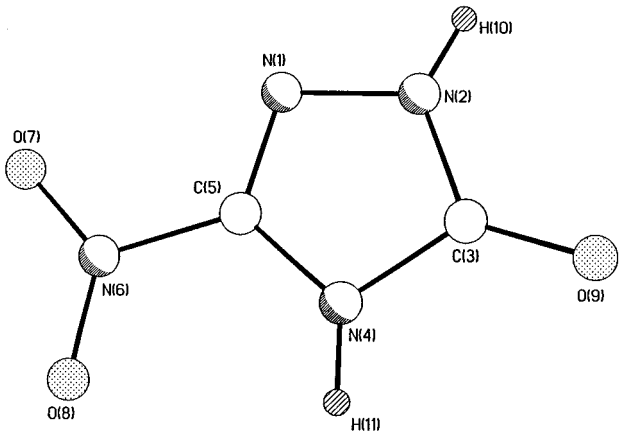

Figure 2. Molecular configuration of NTO. Atom labels are consistent with the indices given in Table 1.

These results suggest that accurate descriptions of the equilibrium properties of the *β*-NTO crystal can be predicted by this intermolecular potential.

B. NPT Molecular Dynamics Calculations. A more realistic prediction of the structural lattice parameters can be obtained by considering the molecular motion as a function of temperature and pressure. For this purpose, we have determined the structural parameters at zero pressure for the temperature range 4.2−400 K.

A typical evolution of the time histories of the lattice parameters (*a*, *b*, *c*, α, *β*, *γ*) and the volume, pressure, and rotational and translational temperatures are given in Figures 3 and 4 for a trajectory calculated for an external temperature of 300 K. The trajectory is well behaved; each property oscillates about the average value for the duration of the trajectory.

The crystal structure information calculated from such trajectories integrated at $T = 4.2$ and 300 K is detailed in Table 5. As can be seen by comparing data in Tables 5A and 3, the lattice dimensions obtained at $T = 4.2$ K are in very close agreement with those determined in the molecular packing calculations without symmetry constraints. This is the expected

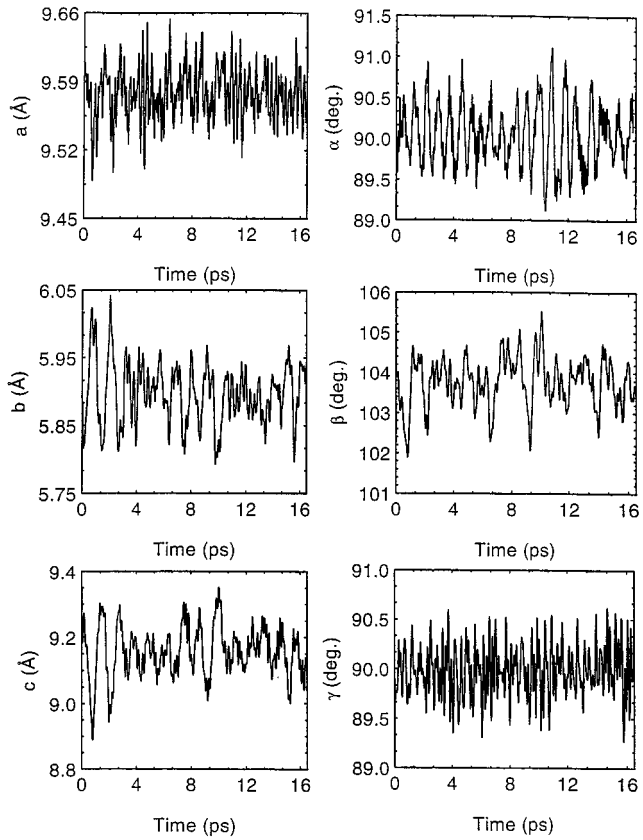

Figure 3. Time histories of lattice parameters (*a*, *b*, *c*, α, *β*, *γ*) for an isothermal−isobaric trajectory corresponding to 300 K and 0 atm.

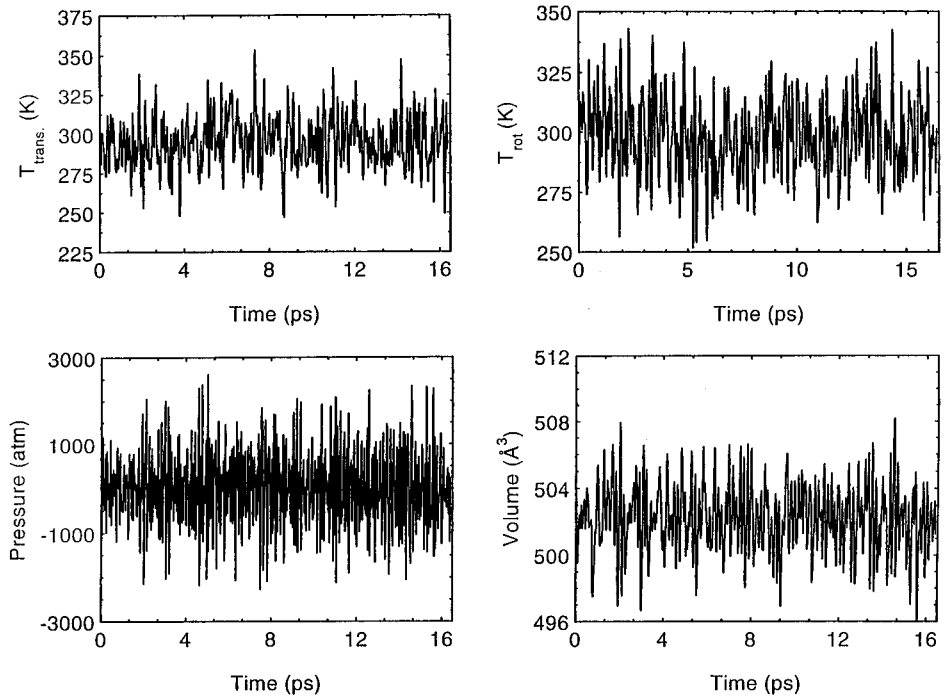

Figure 4. Time histories of the unit cell volume, pressure, rotational temperature (T_{rot}), and center-of-mass translational temperature (T_{trans}) for an isothermal−isobaric trajectory corresponding to 300 K and 0 atm.

TABLE 5: Average Values of the (A) Lattice Dimension, (B) Fractional Coordinates, and (C) Euler Angles (X-Convention[a]) of the Molecular Center-of-Mass Calculated from Trajectories at 4.2 and 300 K; The Corresponding Values Determined for the Experimental Geometry[b] Are Also Given

(A)

	a (Å)		*b* (Å)		*c* (Å)		volume (Å^3)	
temp (K)	MD-NPT	expt	MD-NPT	expt	MD-NPT	expt	MD-NPT	expt
300	9.5773	9.3260	5.8974	5.5150	9.1564	9.1070	502.228	460.148
4.2	9.5763		5.7914		9.0190		484.454	

(B)

	Sx			Sy			Sz		
molecule	4.2 K	300 K	expt	4.2 K	300 K	expt	4.2 K	300 K	expt
1	0.264 055	0.258 983	0.255 585	0.489 712	0.501 617	0.502 656	0.827 007	0.836 225	0.838 046
2	0.735 947	0.741 219	0.744 415	0.989 715	0.001 813	0.002 656	0.672 990	0.663 828	0.661 954
3	0.735 963	0.741 071	0.744 415	0.510 289	0.498 436	0.497 344	0.172 994	0.163 807	0.161 954
4	0.264 035	0.258 727	0.255 585	0.010 285	0.998 133	0.997 344	0.327 008	0.336 140	0.338 046

(C)

	Φ (deg)			Θ (deg)			Ψ (deg)		
molecule	4.2 K	300 K	expt	4.2 K	300 K	expt	4.2 K	300 K	expt
1	178.65	170.02	172.94	34.19	35.25	34.44	77.70	80.72	83.31
2	−178.69	−170.37	−172.94	145.79	144.75	145.55	−102.29	−99.49	−96.68
3	178.63	170.33	172.94	34.19	35.27	34.33	77.71	80.58	83.31
4	−178.68	−170.43	−172.94	145.79	144.73	145.55	−102.28	−99.60	−96.68

[a] Goldstein, ref 48. [b] Lee and Gilardi, ref 15.

result when the potential minimum determined in molecular packing calculations is not a local but rather an absolute minimum, and consequently the molecular configuration found in molecular packing minimization corresponds to the average one determined in molecular dynamics simulations at low levels of thermal energy. At 300 K the average lattice dimensions agree satisfactorily with the experimental values, the corresponding differences for *a*, *b*, and *c* lattice dimensions being 2.69%, 6.93%, and 0.5%, respectively. Moreover, in both low and ambient temperature simulations, the unit cell angles α and γ remain approximately equal to 90°, while the β angle decreases from 104.42° to 103.76°, over the temperature range 4.2−400 K.

In Table 5B,C and in Figure 5 we compare the results of the average fractional coordinates and orientational parameters of the four molecules in the unit cell with the corresponding experimental data. It is evident that increasing the temperature from 4.2 to 300 K does not produce any significant displacement of the molecular center-of-mass (COM) and that the degree of rotational disorder is small. In addition, we observe from Figure 5 that a slightly better agreement exists between the orientational parameters and fractional coordinates of the molecules at 300 K and the experimental values than is the case for those determined at lower temperatures.

Additional support for the small degree of translation of the molecules inside the unit cell with the temperature increase can

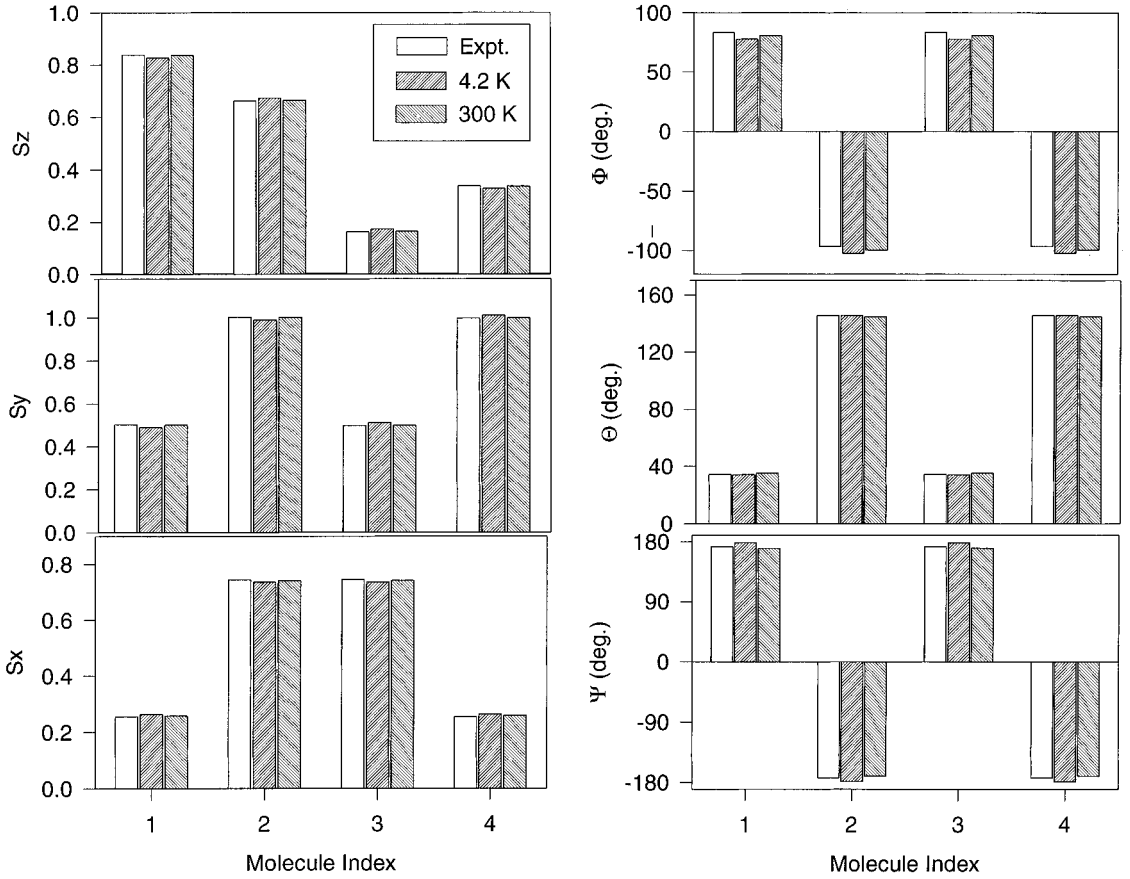

Figure 5. Comparison of time-averaged center-of-mass fractional positions and Euler angles (X-convention[48]) with experiment results at 300 K and 0 atm. These time averages for each molecule in the unit cell are over the 45 unit cells in the simulation box.

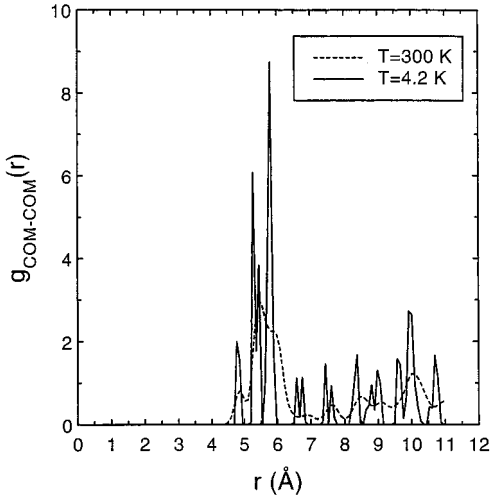

Figure 6. Radial distribution function for center-of-mass−center-of-mass pairs at 4.2 and 300 K.

be obtained from the COM−COM radial distribution functions (RDFs) given in Figure 6. Indeed, the RDFs at these temperatures correspond to well-ordered structures with correlation at long distances. The positions of the major peaks do not change significantly, and the main temperature effect is the broadening of the peaks with partial overlapping of some of them.

Further insight into the stability of intermolecular structure can be obtained by analyzing the site−site RDFs for the case of shorter contacts, *i.e.*, the $O_9\cdots H_{11}$ and $N_1\cdots H_{10}$ intermolecular bonds. These RDFs were calculated as averages over all molecules in the MD box but limited by the cutoff distance used in potential calculation. The results given in Figure 7 show that these short contacts remain at approximately the same

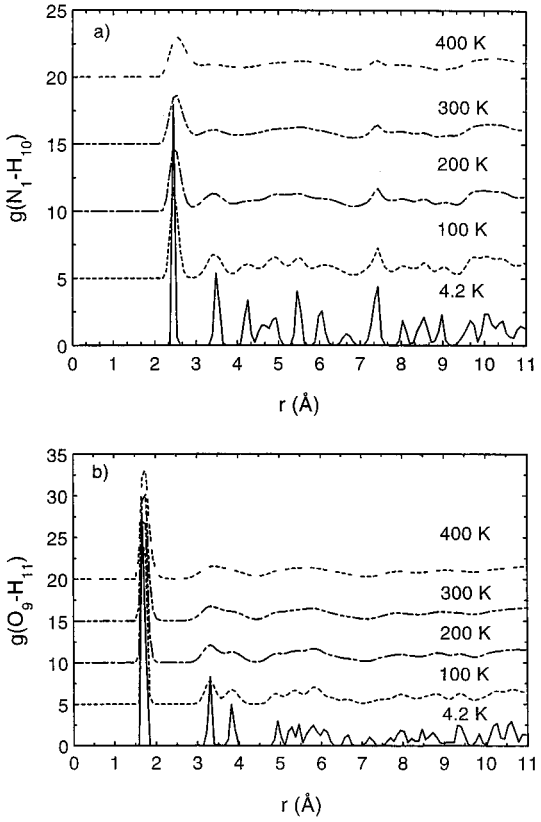

Figure 7. Radial distribution functions for the $H_{11}\cdots O_9$ and $H_{10}\cdots N_1$ pairs as functions of temperature.

average length, particularly in the case of the $C_3{=}O_9\cdots H_{11}-N_4$ hydrogen bond. A much larger increase takes place in the

TABLE 6: NPT-MD Lattice Dimensions at Various Temperatures

T (K)	l_1 (Å)	l_2 (Å)	l_3 (Å)	α	β	γ	volume (Å^3)
4.2	9.5763	5.7914	9.019	89.999	104.425	90.000	484.454
100	9.5815	5.8254	9.0576	90.007	104.253	90.000	489.971
200	9.5756	5.8681	9.0977	90.008	103.958	89.983	496.060
250	9.5732	5.8872	9.1312	89.984	103.887	90.003	499.541
273.15	9.5770	5.8852	9.1626	89.995	103.885	90.004	501.272
300	9.5773	5.8974	9.1564	90.052	103.767	89.981	502.228
325	9.5792	5.9081	9.1784	90.013	103.657	90.013	504.701
350	9.5803	5.91396	9.1960	90.021	103.690	89.997	506.127
375	9.5849	5.9194	9.2218	89.658	103.767	90.032	508.097
400	9.5851	5.9236	9.2471	90.026	103.551	90.023	510.274

case of the $N_1\cdots H_{10}-N_2$ contact, as illustrated by the larger shift and broadening of this peak.

Similar types of results have been obtained by calculating the behavior of the system with increasing temperature over the range 4.2−400 K. These data are summarized in Table 6 for the case of the lattice dimensions. This information can be used to extract the linear (α) and the volumic (β) thermal expansion coefficients, which are defined as

$$\alpha \equiv \frac{1}{X}\left(\frac{\partial X}{\partial T}\right)_P \tag{7}$$

and

$$\beta \equiv \frac{1}{V}\left(\frac{\partial V}{\partial T}\right)_P \tag{8}$$

where X denotes the length of one of the sides of the unit cell.

The evaluation of the partial derivations in eqs 7 and 8 can be done by fitting the data in Table 6 to

$$\chi = \chi_0[1 + \chi_1(T - T_0) + \chi_2(T - T_0)^2] \tag{9}$$

where χ_0 represents, respectively, a, b, c, or V at the reference temperature $T_0 = 300$ K and with the coefficients χ_1 and χ_2 determined by the fit.

The temperature dependence of the unit cell volume and lattice parameters are shown in Figure 8a,b. The symbols in Figure 8 denote the time-averaged values obtained from the trajectories (listed in Table 6), and the lines denote fits of these averages to eq 9. The coefficients of each fit are given in Table 7. Based on these values, the linear expansion coefficients for lattice dimensions a, b, and c are, respectively, 5.0×10^{-6}, 50.7×10^{-6}, and 79.3×10^{-6} K^{-1} at $T = 300$ K, and the corresponding volume expansion coefficient is 142.8×10^{-6} K^{-1}. These values indicate anisotropic thermal behavior of the crystal. Indeed, the thermal variation along the a direction is very small, while the variations along the b and c crystallographic directions are significantly larger. At present, no experimental data are available to which the calculated thermal coefficients can be compared.

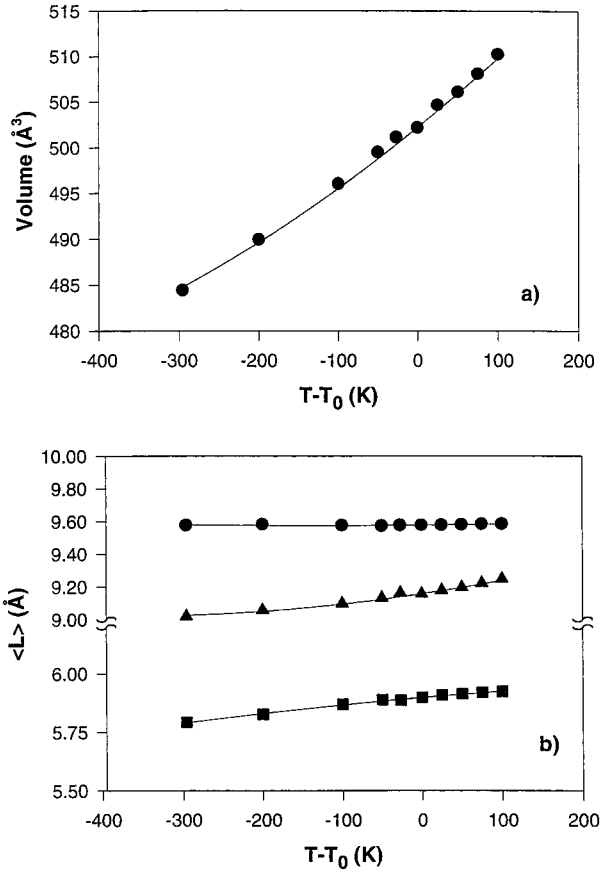

Figure 8. Unit cell volume (a) and cell lengths (b) as functions of temperature. The symbols denote time averages, and the solid curves are linear fits of the points. In frame b the filled circles, squares, and triangles correspond to lattice dimensions a, b, and c, respectively.

TABLE 7: Coefficients of the Quadratic Fit (Eq 7) for the Expansion of the Unit Cell Dimensions and Volume as Functions of Temperature[a]

parameter	χ_0	χ_1	χ_2
a	9.5773	5.0984×10^{-6}	1.9964×10^{-8}
b	5.8974	5.0734×10^{-5}	-3.6415×10^{-8}
c	9.1564	7.9366×10^{-5}	1.0525×10^{-7}
V	502.2287	1.4280×10^{-4}	8.5883×10^{-8}

[a] The reference temperature is $T_0 = 300$ K. The units for the coefficients χ_0, χ_1, and χ_2 are Å, Å/K, and Å/K^2 for a, b, and c, and Å^3, Å^3/K, and Å^3/K^2 for volume V, respectively.

IV. Summary and Conclusions

We have developed an intermolecular potential for the β-form of the NTO crystal based on 6−12 Lennard-Jones potentials, 10−12 hydrogen bond terms, and Coulombic interactions. Electrostatic charges of different atoms in the NTO molecule were determined from fits to *ab initio* electrostatic potentials calculated at the MP2/6-31G** level. Values for several of the homoatom potential parameters were taken from published data[26] and used with the corresponding combination rule (eqs 5 and 6) to generate the heteroatom potential parameters. Only the C═O···H−N hydrogen bond potentials were optimized to minimize the difference between the theoretical and experimental[15] structures and their corresponding energies.

A prime test of the proposed potential was done in symmetry-unconstrained molecular packing calculations. It was shown that the space group symmetry is maintained throughout energy minimization and that the crystallographic parameters are reproduced with an acceptable degree of accuracy. Very good

agreement was obtained for the lattice energy and the estimated enthalpy of sublimation corrected by the 2*RT* term.

The temperature dependencies of the physical parameters of the lattice have been investigated by performing isothermal−isobaric molecular dynamics simulations at zero pressure over the temperature range 4.2−400 K. The results of these calculations indicate that at 300 K the model reproduces the experimental unit cell dimensions within 6.9%. Additionally, little rotational or translational disorder occurs in thermal, unconstrained trajectories.

The linear and volumic thermal expansion coefficients of the crystal were determined from the averages of lattice dimensions extracted from trajectory calculations. The results obtained indicate anisotropic behavior of the crystal with expansions preferentially along the *b* and *c* axes.

This model is useful for predicting nonreactive processes in the β-NTO crystal. Refinement of this model can be made by including the effects of intramolecular motions, particularly of low-frequency torsional motions of the nitro group and of the ring. In addition, the model can be extended to reproduce not only geometry and energy parameters, but also spectroscopic data for the NTO lattice. Further development of the model to include the intramolecular degrees of freedom are expected to facilitate full atomistic investigations of the dynamics of this energetic material.

Acknowledgment. D.C.S. thanks Professor John Yates for his hospitality during the course of this work. This work was supported by the Air Force Office of Scientific Research.

References and Notes

(1) Rothgery, E. F.; Audetter, D, E.; Wedlich, R. C.; Csejka, D. A. *Thermochim. Acta* **1991**, *185*, 235.

(2) Menapace, J. A.; Marlin, J. E.; Bruss, D. R.; Dascher, R. V. *J. Phys. Chem*. **1991**, *95*, 5509.

(3) Östmark, H.; Bergman, H.; G., Åqvist, A. Langlet, and B. Persson, *Proc. Int. Pyrotech. Semin.* **1991**, *16*, 874.

(4) Prabhakaran, K. V.; Naidu, S. R.; Kurian, E. M. *Thermochim. Acta* **1994**, *241*, 199.

(5) Yi, X.; Hu, R.; Wang, X.; Fu, X.; Zhu, C. *Thermochim. Acta* **1991**, *189*, 283.

(6) Oxley, J. C.; Smith, J. L.; Zhou, Z. *J. Phys. Chem*. **1995,** *99*, 10383.

(7) Brill, R. B.; Gongwer, P. E.; Williams, G. K. *J. Phys. Chem*. **1994**, *98*,12242.

(8) Botcher, T. R.; Beardall, D. J.; Wight, C. A.; Fan, L.; Burkey, T. J. *J. Phys. Chem*. **1996,** *100*, 8802.

(9) Sorescu, D. C.; Sutton, T. R. L.; Thompson, D. L.; Beardall, D.; A., C. Wight, *J. Mol. Struct*. **1996**, *384*, 87.

(10) Moller, C. M. S. *Phys. Rev*. **1934**, *46*, 618. Hehre, W. J.; Ditchfield, R.; Pople, J. A. *J. Chem. Phys*. **1972**, *56*, 2257. Hariharan, P. C.; Pople, J. A. *Theor. Chim. Acta* **1973**, *28*, 213. Gordon, M. S. *Chem. Phys. Lett*. **1980**, *76*, 163.

(11) Becke, A. D. *J. Chem. Phys*. **1993**, *98*, 5648.

(12) Lee, C.; Yang, W.; Parr, R. G. *Phys. Rev*. **1988**, *B41*, 785.

(13) Binkley, J. S.; Pople, J. A.; Hehre, W. J. *J. Am. Chem. Soc*. **1980**, *102*, 939.

(14) Krishnan, R.; Frisch, M. J.; Pople, J. A. *J. Chem. Phys*. **1980,** *72*, 4244.

(15) Lee, K.-Y.; Gilardi, R.; In *Structure and Properties of Energetic Materials*; Lienbenberg, D. H.; Armstrong, R. W.; Gilman, J. J. Eds.; Materials Research Society: Pittsburgh, PA, 1993); Vol. 296, p 237.

(16) Sorescu, D. C.; Rice, B. M.; Thompson, D. L. *J. Phys. Chem*. **1997**, *101*, 798.

(17) Pertsin, A. J.; Kitaigorodsky, A. I. *The Atom-Atom Potential Method, Applications to Organic Molecular Solids*; Springer-Verlag: Berlin, 1987.

(18) Desiraju, G. R. *Crystal Engineering: The Design of Organic Solids*; Elsevier: Amsterdam, 1989.

(19) Weiner, S. J.; Kollman, P. A.; Nguyen, D. T.; Case, D. A. *J. Comput. Chem*. **1986**, *7*, 230.

(20) Nemethy, G.; Gibson, K. D.; Palmer, K. A.; Yoon, C. N.; Paterlini, G.; S., Rumsey, and H. A. Scheraga, *J. Phys. Chem*. **1972**, *96*, 6474.

(21) Mayo, S. L.; Olafson, B. D.; Goddard, W. A., III. *J. Phys. Chem*. **1990**, *94*, 8897.

(22) Busing, W. R. *WMIN*, A computer Program to Model Molecules and Crystals I, Terms of Potential Energy Functions; ORNL-5747; Oak Ridge National Laboratory: Oak Ridge, 1981.

(23) Williams, D. E.; In *Crystal Cohesion and Confirmational Energies*; Metzger, R. M., Ed.; Springer-Verlag: Berlin, 1981; pp 3−40.

(24) Williams, D. E. *PCK91*, A Crystal Molecular Packing Analysis Program; Department of Chemistry, University of Louisville: Louisville, KY 40292, 1991.

(25) (a) Hagler, A. T.; Lifson, S.; Dauber, P. *J. Am. Chem. Soc*. **1979**, *101*, 5122. (b) Hagler, A. T.; Dauber, P.; Lifson, S. *J. Am. Chem. Soc*. **1979**, *101*, 5131.

(26) Gibson, K. D.; Scheraga, H. A. *J. Phys. Chem*. **1995**, *99*, 3752.

(27) Gibson, K. D.; Scheraga, H. A. *LMIN*: A Program for Crystal Packing, QCPE No. 664.

(28) Gay, D. M. *ACM Trans. Math. Software* **1983,** *9*, 503.

(29) *International Tables for Crystallography*; Hahn, T., Ed.; Reidel: Dordrecht, Boston, 1983.

(30) *Fundamentals of Crystallography*; Giacovazzo, C., Ed.; Oxford University Press: New York, 1992.

(31) Ritchie, J. P. *J. Org. Chem*. **1989**, *54*, 3553.

(32) Ibrahim, M. R.; Schleyer, P. R. *J. Comput. Chem*. **1985,** *6*, 157.

(33) Politzer, P.; Murray, J. S.; Grice, M. E. *Mater. Res. Soc. Symp*. **1996**, *418*, 55.

(34) Finch, A.; Gardner, P. J.; Head, A. J.; Majdi, H. S. *J. Chem. Thermodyn.* **1991**, *23*, 1169.

(35) See, for example, See, for example, Wiberg, K. B.; Rablen, P. R. *J. Comput. Chem*. **1993**, 14, 1504, and references therein.

(36) Breneman, C. M.; Wiberg, K. B. *J. Comput. Chem*. **1990**, *11*, 361.

(37) Frisch, M. J.; Trucks, G. W.; Schlegel, H. B.; Gill, P. M. W.; Johnson, B. G.; Robb, M. A.; Cheeseman, J. R.; Keith, T.; Patersson,G. A.; Montgomery, J. A.; Raghavachari, K.; AL-Laham, M. A.; Zakrzewski, V. G.; Ortiz, J. V.; Foresman, J. B.; Cioslowski, J.; Stefanov, B. B.; Nanyakkara, A.; Challacombe, M.; Peng, C. Y.; Ayala, P. Y.; Chen, W.; Wong, M. W.; Andres, J. L.; Replogle, E. S.; Gomperts, R.; Martin, R. L.; Fox, D. J.; Binkley, J. S.; Defrees, D. J.; Baker, J.; Stewart, J. P.; Head-Gordon, M.; Gonzales, C.; Pople, J. A. *Gaussian 94*, Revision C.3; Gaussian, Inc.: Pittsburgh, PA, 1995.

(38) (a) Hehre, W. J.; Ditchfield, R.; Pople, J. A. *J. Chem. Phys*. **1972**, *56*, 2257. (b) Frankl, M. M.; Pietro, W. J.; Hehre, W. J.; Binkley, J. S.; Gordon, M. S.; DeFrees, D. J.; Pople, J. A. *J. Chem. Phys*. **1982**, *77*, 3654.

(39) Andersen, H. C. *J. Chem. Phys*. **1980**, *72*, 2384.

(40) Parrinello, M.; Rahman, A. *Phys. Rev. Lett*. **1980**, *45*, 1196.

(41) Klein, M. L. *Annu. Rev. Phys. Chem*. **1985**, *36*, 525.

(42) Nosé, S.; Klein, M. L. *Mol. Phys*. **1983,** *50*, 1055.

(43) Nosé, S.; Klein, M. L. *J. Chem. Phys*. **1983**, *78*, 6928.

(44) W. Smith, *MDSCPC4B*, A Program for Molecular Dynamics Simulations of Phase Changes; CCP5 Program Library (SERC), May 1991.

(45) Gear, C. W. *Numerical Initial Value Problems in Ordinary Differential Equations* Prentice-Hall, Princeton, NJ, 1971.

(46) Evans, D. J. *Mol. Phys*. **1977**, *34*, 317.

(47) Allen, M. P.; Tindesley, D. J. *Computer Simulation of Liquids*; Oxford University Press: New York, 1989.

(48) Goldstein, H. *Classical Mechanics*; Addison-Wesley: Reading, MA, 1980.